Wiley Online Library
Early View publication on www.wileyonlinelibrary.com
(issue and page numbers not yet assigned;
citable using Digital Object Identifier – **DOI**)

Phys. Status Solidi A, 1700263 (2017) / **DOI** 10.1002/pssa.201700263

physica status solidi a
www.pss-a.com
applications and materials science

Density functional theory calculations of helium clustering in mono-, di-, and hexa-vacancy in silicon

Laurent Pizzagalli,*,[1] Marie-Laure David,[1] and Julien Dérès[1]

[1] Institut Pprime, UPR3346 CNRS-Université de Poitiers, 86962 Futuroscope-Chasseneuil, France

Received 10 April 2017, revised 26 April 2017, accepted 26 April 2017
Published online 5 June 2017

Keywords DFT, Helium, silicon, vacancies

* Corresponding author: e-mail Laurent.Pizzagalli@univ-poitiers.fr, Phone: +33549497499, Fax: +33549496692

Combining classical molecular dynamics and first-principles DFT calculations, we perfom an extensive investigation of low energy configurations for He_nV_m complexes in silicon. The optimal helium fillings are hence determined for V_1, V_2, and V_6 (figure on the right), and the structures formed by helium atoms arrangements in the vacancy defect are analyzed. For V_1 and V_2, the He atoms structure is mainly controled by the host silicon matrix, whereas a high density helium packing is obtained for V_6. For the latter, we estimate a helium density of about 170 He nm^{-3} in the center of the hexa-vacancy at the optimal helium filling.

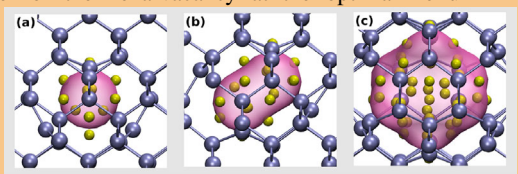

Relaxed structures obtained from DFT calculations for configurations with the lowest formation energies: (a) $He_{14}V_1$, (b) $He_{20}V_2$, and (c) $He_{40}V_6$.

1 Introduction The formation of noble gas bubbles in materials has been the focus of numerous investigations, motivated by the will to understand and control the influence of these bubbles on materials properties. Most of the available studies were dedicated to the state of already formed bubbles, and on their evolution during coarsening stages [1–9]. Another important information regarding these bubbles relates to the very first steps leading to the formation, that is, the aggregation of noble gas impurities and how the latter interact with point defects like vacancies or self-interstitials. Several investigations have been conducted in metals [10–15], in particular because of their importance in nuclear applications.

In semiconductors, fewer works are available, and typically focus on helium in silicon or in silicon carbide. Theoretical investigations revealed that in the undefected cubic diamond lattice, an interstitial helium atom is located in tetrahedral sites [16–23] and diffuses through hexagonal sites [19, 22, 24]. It has also been shown that helium interstitials do not easily cluster [16, 25, 26], thus highlighting the pivotal role of vacancies in the initial stages of helium bubbles formation. Much less information is available regarding the aggregation of helium atoms and vacancies. For the smallest systems, first principles calculations revealed a repulsive interaction between one helium atom and a mono-vacancy [16, 17]. Thus, the first stable complex seems to be composed of one helium atom positioned into a di-vacancy [18, 23]. Experiments also point to the importance of di-vacancies during the formation of helium bubbles in silicon [4, 27, 28] and in silicon carbide [29].

The lack of knowledge between an elementary complex composed of one helium atom and a di-vacancy, and a nanometric sized bubble is consequent, and additional studies of helium-vacancy complexes are obviously needed. For instance, we do not know whether extra helium atoms could be easily inserted into a di-vacancy, or how many could be incorporated into larger voids. Recently, partial answers were provided by a theoretical investigation in silicon carbide, which revealed that a maximum amount of 14 helium atoms can be incorporated into a 7-vacancies void in silicon carbide [30]. In this work, initial helium positions are however restricted to interstitial sites, which could lead to an underestimation of the optimal helium filling. Our goal is to perform a similar investigation in silicon, with no such restriction.

2 Methods We aim at determining the most stable configuration when n helium atoms are inserted into a mono-vacancy (V_1), a di-vacancy (V_2), and an hexa-vacancy (V_6) in silicon. This selection is motivated by the important role of V_1 and V_2 as primary defects, and the high stability of V_6 in silicon. Also, we implicitely assume here that the formation of these vacancy-like clusters precede that of the He_nV_m aggregates, as recently reported [31]. Finding the energetically most stable configuration is a non-trivial problem because of the large number of possible candidates for $n > 1$. To tackle this issue, the following strategy is adopted: (i) a large set of quenched classical molecular dynamics is first performed for each n, starting from various initial helium atoms configurations (ii) best candidates, that is, with the lowest energies, are then used as input in Density Functional Theory (DFT) calculations. Although such a procedure can not guarantee that the global energy mininum is found in each case, it allows for an efficient exploration of the configuration space. It also does not assume that helium atoms are initially positioned at interstitial sites, as in previous works [30].

The first set of simulations is performed using the LAMMPS package [32]. The silicon–helium system is described with a Modified Embedded Atom Method (MEAM) potential, which was specifically developed to reproduce properties of helium in silicon [31]. With this potential, the silicon lattice parameter is $a_0 = 5.431$ Å. V_1, V_2, and V_6 are built by removing selected atoms in a periodically repeated $(4a_0)^3$ supercell, thus containing initially 512 Si atoms, followed by a conjugate gradients relaxation. In the case of V_6, a ring-like structure is considered as initial structure, since it has been shown to be a low energy configuration [33].

Helium atoms are then inserted in a spherical region of variable radius and centered on the vacancies, according to three different methods. In the first one, a piece of helium HCP crystal is inserted in the as-created void, its density being adjusted to get the desired number of He atoms. In the second one, the helium atoms are randomly inserted into the void. The third method is a variant of the previous one, with some of the He atoms randomly positioned in tetrahedral sites in the immediate vicinity of the vacancies. In all cases, the initial separations between the atoms are computed before the molecular dynamics simulations, and configurations with strongly overlapping atoms are discarded.

Each initial configuration is then relaxed using conjugate gradients, followed by a 300 K molecular dynamics simulations during 3 ps, the elementary time step being 1 fs. This stage allows for an efficient reordering, while keeping the helium atoms inside or in the vicinity of the cavity. Finally, the system is again relaxed using conjugate gradients. This procedure is repeated at least fifty times for each He_nV_m case by using a python script which (i) automatically generates new initial configurations (ii) calls the LAMMPS atomistic calculations. The best candidates, that is, with the lowest energies, are then used as input in DFT calculations.

These calculations are done using the Quantum Espresso package [34], using a plane waves basis cut-off of 15 Ry and ultrasoft Vanderbilt pseudopotentials [35]. The Perdew–Burke–Ernzerhof functional is used to describe exchange-correlation contributions [36]. The complexes configurations previously obtained are trimmed and scaled to fit in a $(3a_0)^3$ supercell, that is, including $N = 216$ atoms for pristine bulk, with $a_0 = 5.468$ Å. A $\frac{1}{2}$-shifted 2^3 Monkhorst-Pack grid of k-points [37] is used to sample the Brillouin zone. A conjugate gradients relaxation is performed until the largest ionic force is below 2×10^{-3} eV Å^{-1}.

In the following, the formation energy of V_m is calculated according to the usual definition

$$E_f(V_m) = E(V_m) - \frac{N-m}{N} E_0 \tag{1}$$

with $E(V_m)$ and E_0 the total energies of V_m and silicon bulk, respectively, computed in the same supercell. In the presence of helium, we define the formation energy of the $E_f(He_nV_m)$ cluster as the energy change when n He atoms in isolated interstitial configurations are inserted into V_m:

$$E_f(He_nV_m) = E(He_nV_m) - E(V_m) - nE_f(He) \tag{2}$$

with $E(He_nV_m)$ the total energy of He_nV_m, and $E_f(He)$ the formation energy of a tetrahedral interstitial helium atom. The latter is computed to be 0.9924 eV. A negative formation energy then indicates that it is energetically favorable for the n helium atoms to be located in the V_m defect rather than in interstitial sites. We also define the binding energy E_b as the energy change when an interstitial helium atom is added to a He_nV_m complex:

$$\begin{aligned} E_b(He_{n+1}V_m) &= E(He_{n+1}V_m) - E(He_nV_m) - E_f(He) \\ &= E_f(He_{n+1}V_m) - E_f(He_nV_m) \end{aligned} \tag{3}$$

3 Results We first validate our calculations by comparing the results for $V_{m=1,2,6}$ with earlier calculations. For V_1, the formation energy is equal to 3.33 eV, in excellent agreement with reference works [38, 39]. Also the relaxed structure is characterized by the correct D_{2d} symmetry [39]. For V_2, we obtain 5.05 eV, yielding a dissociation energy $E_f(V_2) - 2E_f(V_1)$ equal to 1.72 eV, again in excellent agreement with previous works [40, 41]. Finally, we compute $E_f(V_6) = 8.61$ eV, which is about 1 eV lower than values reported in the literature [42, 43]. It is difficult to explain such a difference, except that maybe our electronic structure calculations are better relaxed than in these early works.

Considering now vacancies, our simulations reveal that inserting a single helium atom into V_1 is not energetically favorable, with $E_f = 0.15$ eV if He is located in a tetrahedral site first-neighbor of the vacancy, and $E_f = 0.82$ eV if

it is positioned in the vacancy center. The repulsive nature of the V_1 center for helium is due to an electronic effect and is a well documented fact in the literature [16, 17, 23]. Adding further helium atoms, a negative formation energy is obtained (Fig. 1). The first stable helium-vacancy complex is He_2V_1, with a formation energy of –0.1 eV. In the relaxed geometry, the two helium atoms are separated by 1.9 Å, and aligned along a ⟨110⟩ direction. They are also both located 1.57 Å away from the vacancy center, again because of the electronic repulsion at vacancy center. However, with three He atoms in the vacancy, this effect is overcome by the need to accomodate the extra helium atoms. The latter then forms a triangular structure approximately contained in a (111) plane (Fig. 2). For this configuration, E_f is equal to –0.34 eV. Figure 2 shows the helium atoms arrangement for few other selected cases. It clearly appears that the helium atoms form ordered patterns. In the case of V_1, the available volume is small and helium atoms packing coherent with the cubic diamond lattice is favored. At the highest content, the structure is composed of a high density helium configuration at the vacancy center, surrounded by helium atoms approximately in first neighbors tetrahedral sites. This is the case for instance of $He_{14}V_1$ which corresponds to the lowest formation energy $E_f = -3.95$ eV for He_nV_1 complexes (structure shown in Fig. 3).

Considering now V_2, we find $E_f = -0.50$ eV for He_1V_2 in agreement with previous works [17, 23]. For He_2V_2, the most stable configuration ($E_f = -0.36$ eV) corresponds to two helium atoms approximately aligned along ⟨111⟩, and centered on one vacancy. This preference for helium atoms to group together in a single vacancy is also obtained for He_3V_2, with a triangular arrangement centered on one vacancy. However, for $n > 3$, both vacancy centers become occupied by helium atoms. Figure 2 represents three examples

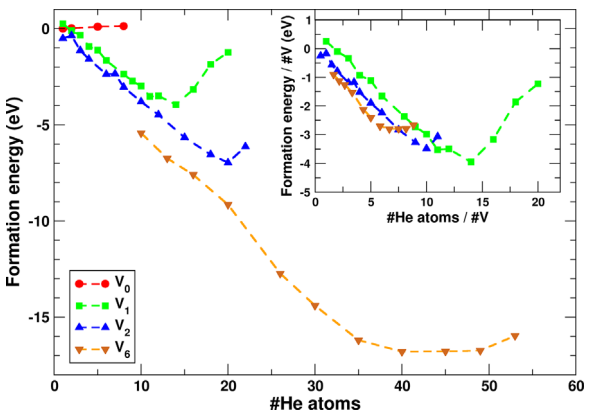

Figure 1 Formation energy (as defined in Eq. (2)) as a function of the number of helium atoms in $V_{m=1,2,6}$, from DFT calculations. Each symbol corresponds to a calculation, whereas dashed lines are drawn to show trends. In red is also reported the formation energy variation corresponding to helium interstitial aggregation in the pristine silicon bulk [26]. The inset graph represents the same information, but now normalized with respect to the number of vacancies along the two axis.

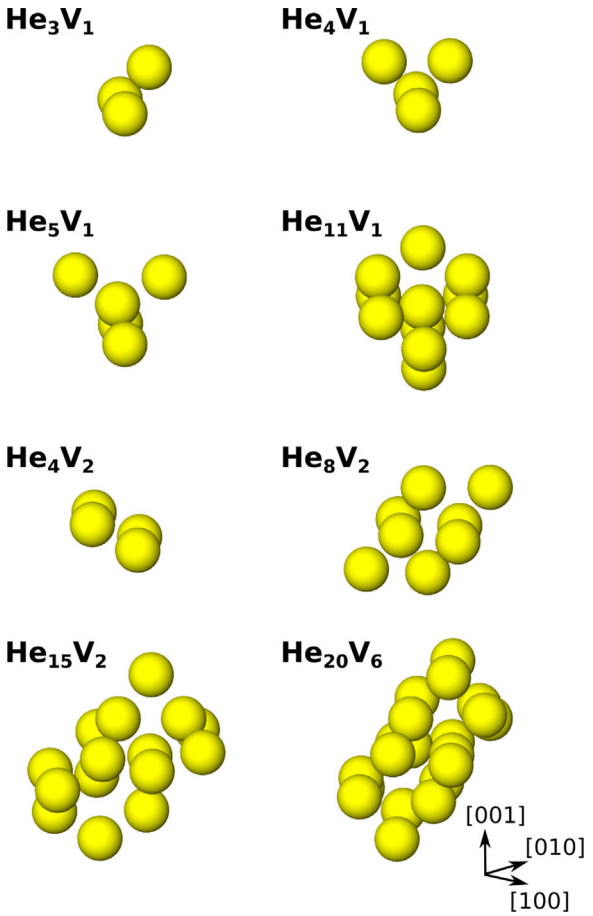

Figure 2 Atomistic representations of relaxed helium geometries obtained from DFT calculations for selected configurations. Only He atoms are represented (yellow spheres with arbitrary radii) for clarity.

of helium atoms packing into V_2. In particular, one can see that He_8V_2 is geometrically equivalent to He_4V_1. The lowest calculated formation energy is –6.97 eV, and corresponds to $He_{20}V_2$ with the configuration shown in Fig 3.

For V_6, the larger available volume obviously allows for an energetically favorable filling with helium atoms, and only the cases with at least ten helium atoms are investigated. Overall, we first observe that the helium atoms tend to spread over the largest possible space, with no well-defined ordering. When about twenty helium atoms are present in V_6, the configuration becomes more ordered, probably because of the increasing internal pressure. The He atoms tend to pack themselves in the two $\{111\}$ planes containing the vacancies (Fig. 2). The lowest formation energy $E_f = -16.795$ eV is obtained for $He_{40}V_6$ (Fig. 3). As for $He_{20}V_2$, the corresponding geometry is characterized by a central region with a high density of helium atoms, and an outer shell of helium approximately located in tetrahedral sites. A structural analysis suggests that ordered patterns might be present in the helium cluster core, several helium atoms exhibiting features associated with icosahedral and HCP structures. However, there are too few atoms to allow for a quantitative analysis.

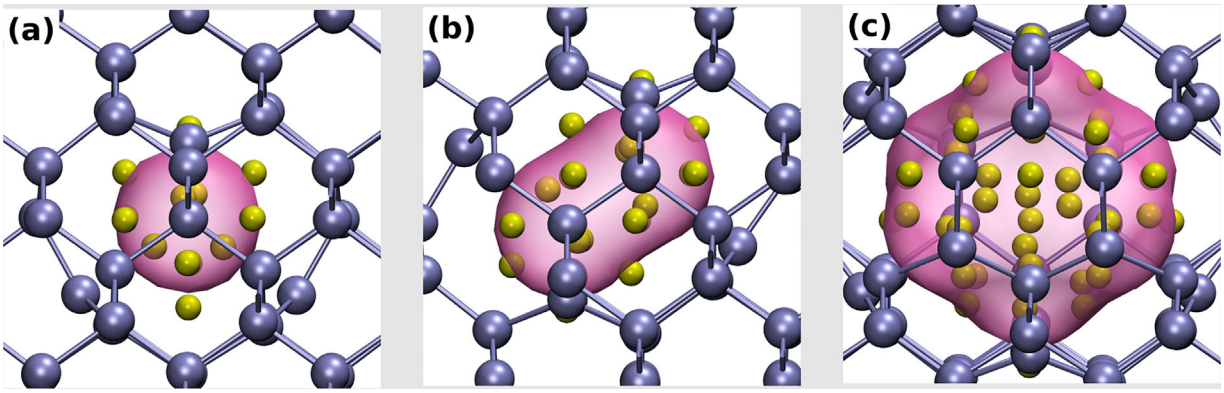

Figure 3 Atomistic representations of relaxed structures obtained from DFT calculations for configurations with the lowest formation energies: (a) $He_{14}V_1$ (b) $He_{20}V_2$, and (c) $He_{40}V_6$. Si (He) atoms are represented by blue (yellow) spheres with arbitrary radii. The vacancies are schematically shown as a pink cloud (Note that the extension of the cloud is not a measure of the cavity volume associated with vacancies).

The He_nV_m formation energy curves plotted in Fig. 1 show a similar variation as a function of n, that is, a decrease to a minimum value at n_{min}, followed by an increase. At low n, the energy is lowered when interstitial He atoms are transferred in the empty volume provided by vacancies. Larger helium aggregates implies pressure building up inside the cavity, and the associated energy cost explains the formation energy increasing above a threshold helium density. Note that by definition a negative formation energy value means that He clustering in V_m is favored, even for $n > n_{min}$. However, helium atoms can not be introduced all together in a single move in V_m, and it is physically more meaningful to consider the successive introduction of helium atoms. The energy change associated with this process is the binding energy E_b defined in Eq. (3), and it is negative only for $n < n_{min}$. The formation energy minimum then corresponds to the optimal helium filling occuring during a physically realistic process.

The optimal filling is reached at $n_{min} = 14, 20, 40$ for V_1, V_2, and V_6 respectively. These values are comparable to the optimal helium fillings found in vanadium [13], but are significantly higher than predictions made for silicon carbide [30, 44]. It has also been suggested that not all helium atoms are strictly encompassed in the empty volume associated with vacancies in SiC [44]. It is also found here that a significant amount of the helium atoms bound in He_nV_m are approximately located in the tetrahedral sites first-neighbors of the vacancies, as seen in Fig. 3. Furthermore, we try to determine the properties of bubble-like systems by extrapolating our results to larger He_nV_m complexes. The inset graph in Fig. 1 shows the formation energies variations for He_nV_m normalized on both axis by m. For $He_{40}V_6$, the He/V ratio is 6.66 and the associated energy is –2.80 eV per vacancy. Unfortunately, larger V_m cavities are seemingly required for a meaningful extrapolation.

Finally, we propose to estimate the helium density by determining the volume of helium atoms in the center of the He_nV_m complex. A good approximation is given by the Voronoi atomic volume, provided all neighbors to the considered atoms are helium and not silicon atoms. There are two such helium atoms in the case of $He_{40}V_6$, with atomic volumes equal to 5.82 Å^3 and 6.04 Å^3. This corresponds to helium densities of 172 and 165 He nm^{-3} and an internal pressure of about 19 GPa [45], which is surprisingly close to the range of values measured in nanometric-sized bubbles [9, 46].

4 Conclusions This paper reports theoretical investigations of helium clustering in vacancy-like defects in silicon, in order to better understand the properties of He_nV_m complexes as precursors of helium-filled bubbles. For each (n,m) couple, a large set of configurations is first explored using classical molecular dynamics. The most promising candidates are then relaxed using first-principles calculations. While this procedure cannot guarantee that the absolute energy minimum is found in each case, it is a significant improvement compared to previous works where helium atoms were initially only inserted in interstitial sites.

For V_1 and V_2, we find that at low content, the He atoms tend to avoid vacancy centers, where the electronic density is non-negligible. At higher content, helium atoms are organized in geometries coherent with the host silicon lattice. For V_6, high density packings optimizing the available space are obtained. We determine optimal helium fillings of 14, 20, 40 for V_1, V_2, and V_6 respectively, using an energetic criterion. A significant proportion of these helium atoms are not contained in the available volume associated to vacancies, but are located in tetrahedral sites first neighbor of the V_m cluster. In the center of V_6, the helium density is estimated to be 165–172 He nm^{-3}.

We emphasize that these calculations are performed at 0 K and in small supercells, because of the computational cost of DFT calculations. Thermal effects should have a significant influence on the state of these He_nV_m clusters. For instance, relaxation mechanisms of the silicon matrix at such high helium densities could be thermally activated.

This probably defines the main research direction for future investigations.

References

[1] H. Trinkaus, Radiat. Eff. **78**, 189, 1983.
[2] G. F. Cerofolini, F. Corni, S. Frabboni, C. Nobili, G. Ottaviani, and R. Tonini, Mater. Sci. Eng. R **27**, 1, 2000.
[3] M. F. Beaufort, E. Oliviero, H. Garem, S. Godey, E. Ntsoenzok, C. Blanchard, and J. F. Barbot, Philos. Mag. B **80**, 1975, 2000.
[4] M. L. David, M. F. Beaufort, and J. F. Barbot, J. Appl. Phys., **93**, 1438, 2003.
[5] S. Frabboni, F. Corni, C. Nobili, R. Tonini, and G. Ottaviani, Phys. Rev. B **69**, 165209, 2004.
[6] S. M. Valones, M. I. Baskes, and R. L. Martin, Phys. Rev. B **73**, 214209, 2006.
[7] S. M. Hafez Haghighat, G. Lucas, and R. Schäublin, Europhys. Lett. **85**, 60008, 2009.
[8] S. Fréchard, M. Walls, M. Kociak, J. Chevalier, J. Henry, and D. Gorse, J. Nucl. Mater. **393**, 102, 2009.
[9] J. Dérès, M.-L. David, K. Alix, C. Hébert, D. T. L. Alexander, and L. Pizzagalli, unpublished (2017).
[10] K. Morishita, R. Sugano, B. D. Wirth, and T. D. de la Rubia, Nucl. Instrum. Meth. B **202**, 76, 2003.
[11] C.-C. Fu and F. Willaime, Phys. Rev. B **72**, 064117, 2005,
[12] T. Seletskaia, Y. Osetsky, R. Stoller, and G. Stocks, J. Nucl. Mater. **351**, 109, 2006.
[13] R. Li, P. Zhang, C. Zhang, X. Huang, and J. Zhao, J. Nucl. Mater. **440**, 557, 2013.
[14] J. Boisse, C. Domain, and C. S. Becquart, J. Nucl. Mater. **455**, 10, 2014.
[15] A. Abhishek, M. Warrier, R. Ganesh, and A. Caro, J. Nucl. Mater. **472**, 82, 2016.
[16] M. Alatalo, M. J. Puska, and R. M. Nieminen, Phys. Rev. B **46**, 12806, 1992.
[17] S. K. Estreicher, J. Weber, A. Derecskei-Kovacs, and D. S. Marynick, Phys. Rev. B **55**, 5037, 1997.
[18] V. G. Zavodinsky, A. A. Gnidenko, A. Misiuk, and J. Bak-Misiuk, Vacuum **78**, 247, 2005.
[19] R. M. V. Ginhoven, A. Chartier, C. Meis, W. J. Weber, and L. R. Corrales, J. Nucl. Mater. **348**, 51, 2006.
[20] A. Charaf Eddin, G. Lucas, M. F. Beaufort, and L. Pizzagalli, Comp. Mater. Sci. **44**, 1030, 2009.
[21] W. Cheng, M. J. Ying, F.-S. Zhang, H. Y. Zhou, and S.-F. Ren, Nucl. Instrum. Meth. B **269**, 2067, 2011.
[22] A. Charaf Eddin and L. Pizzagalli, J. Nucl. Mater. **429**, 329, 2012.
[23] L. Pizzagalli, A. Charaf-Eddin, and S. Brochard, Comp. Mater. Sci. **95**, 149, 2014.
[24] L. Pizzagalli and A. Charaf-Eddin, Semicond. Sci. Tech. **30**, 085022, 2015.
[25] J. H. Kim, Y. D. Kwon, P. Yonathan, I. Hidayat, J. G. Lee, J.-H. Choi, and S. C. Lee, J. Mater. Sci. **44**, 1828, 2009.
[26] L. Pizzagalli, M. L. David, and A. Charaf-Eddin, Nucl. Instrum. Meth. B **352**, 152, 2015.
[27] V. Raineri, S. Coffa, E. Szilágyi, J. Gyulai, and E. Rimini, Phys. Rev. B **61**, 937, 2000.
[28] M. David, A. Ratchenkova, E. Oliviero, M. Denanot, M. Beaufort, A. Declémy, C. Blanchard, N. Gerasimenko, and J. Barbot, Nucl. Instrum. Meth. B **198**, 83, 2002.
[29] F. Linez, E. Gilabert, A. Debelle, P. Desgardin, and M. F. Barthe, J. Nucl. Mater. **436**, 150, 2013.
[30] R. Li, W. Li, C. Zhang, P. Zhang, H. Fan, D. Liu, L. Vitos, and J. Zhao, J. Nucl. Mater. **457**, 36, 2015.
[31] L. Pizzagalli, M. L. David, and M. Bertolus, Model. Simul. Mater. Sci. Eng. **21**, 065002, 2013.
[32] S. Plimpton, J. Comput. Phys. **117**, 1, 1995.
[33] J. L. Hastings, S. K. Estreicher, and P. A. Fedders, Phys. Rev. B **56**, 10215, 1997.
[34] P. Giannozzi, S. Baroni, N. Bonini, M. Calandra, R. Car, C. Cavazzoni, D. Ceresoli, G. L. Chiarotti, M. Cococcioni, I. Dabo, A. Dal Corso, S. de Gironcoli, S. Fabris, G. Fratesi, R. Gebauer, U. Gerstmann, C. Gougoussis, A. Kokalj, M. Lazzeri, L. Martin-Samos, N. Marzari, F. Mauri, R. Mazzarello, S. Paolini, A. Pasquarello, L. Paulatto, C. Sbraccia, S. Scandolo, G. Sclauzero, A. P. Seitsonen, A. Smogunov, P. Umari, and R. M. Wentzcovitch, J. Phys-Condens. Matter **21**, 395502, 2009.
[35] D. Vanderbilt, Phys. Rev. B **41**, 7892, 1990.
[36] J. P. Perdew, K. Burke, and M. Ernzerhof, Phys. Rev. Lett. **77**, 3865, 1996.
[37] H. J. Monkhorst and J. D. Pack, Phys. Rev. B **13**, 5188, 1976.
[38] S. Dannefaer, P. Mascher, and D. Kerr, Phys. Rev. Lett. **56**, 2195, 1986.
[39] M. J. Puska, S. Pöykkö, M. Pesola, and R. M. Nieminen, Phys. Rev. B **58**, 1318, 1998.
[40] G. S. Hwang and W. A. Goddard, Phys. Rev. B **65**, 233205, 2002.
[41] D. Caliste and P. Pochet, Phys. Rev. Lett. **97**, 135901, 2006.
[42] D. V. Makhov and L. J. Lewis, Phys. Rev. Lett. **92**, 255504, 2004.
[43] S. Lee and G. S. Hwang, Phys. Rev. B **77**, 085210, 2008.
[44] A. Couet and J. P. Crocombette, and A. Chartier, J. Nucl. Mater. **404**, 50, 2010.
[45] P. Loubeyre, R. LeToullec, J. P. Pinceaux, H. K. Mao, J. Hu, and R. J. Hemley, Phys. Rev. Lett. **71**, 2272, 1993.
[46] K. Alix, M.-L. David, G. Lucas, D. T. Alexander, F. Pailloux, C. Hébert, and L. Pizzagalli, Micron **77**, 57, 2015.